

**A simulation study of the kinetics of passage of CO<sub>2</sub> and N<sub>2</sub> through the liquid/vapor interface of water**

T. Somasundaram, M. in het Panhuis, R. M. Lynden-Bell, and C. H. Patterson

Citation: *The Journal of Chemical Physics* **111**, 2190 (1999); doi: 10.1063/1.479491

View online: <http://dx.doi.org/10.1063/1.479491>

View Table of Contents: <http://scitation.aip.org/content/aip/journal/jcp/111/5?ver=pdfcov>

Published by the [AIP Publishing](#)

---

**Articles you may be interested in**

[Effect of Cu<sub>3</sub>Sn coatings on electromigration lifetime improvement of Cu dual-damascene interconnects](#)  
*Appl. Phys. Lett.* **87**, 211103 (2005); 10.1063/1.2132536

[Diffusion and electromigration of copper in SiO<sub>2</sub>-passivated single-crystal aluminum interconnects](#)  
*Appl. Phys. Lett.* **74**, 37 (1999); 10.1063/1.123125

[A spectroscopic study of the fullerene/metal interface in C<sub>60</sub>-Al multilayers](#)  
*AIP Conf. Proc.* **442**, 265 (1998); 10.1063/1.56526

[Laser microscopy of CoSi<sub>2</sub> formation reaction at the CoSi/Si interface](#)  
*AIP Conf. Proc.* **418**, 457 (1998); 10.1063/1.54667

[Growth of TiSi<sub>2</sub> from codeposited TiSi<sub>x</sub> layers and interfacial layers](#)  
*Appl. Phys. Lett.* **70**, 2386 (1997); 10.1063/1.118880

---



## Re-register for Table of Content Alerts

Create a profile.



Sign up today!



# A simulation study of the kinetics of passage of CO<sub>2</sub> and N<sub>2</sub> through the liquid/vapor interface of water

T. Somasundaram

*Atomistic Simulation Group and Irish Centre for Colloid Science, School of Mathematics and Physics, The Queen's University, Belfast BT7 1NN, United Kingdom*

M. in het Panhuis<sup>a)</sup>

*Department of Physics, Trinity College, Dublin 2, Republic of Ireland*

R. M. Lynden-Bell

*Atomistic Simulation Group and Irish Centre for Colloid Science, School of Mathematics and Physics, The Queen's University, Belfast BT7 1NN, United Kingdom*

C. H. Patterson

*Department of Physics, Trinity College, Dublin 2, Republic of Ireland*

(Received 9 March 1999; accepted 6 May 1999)

The rate of passage of molecules of carbon dioxide and nitrogen through the vapor–liquid interface of water at 300 K is studied by simulation. Previous work has established the form of the free energy profile which has a minimum when the solute molecule is on the surface and a barrier between this state and solution in the bulk liquid. In one set of simulations, trajectories were initiated in the gas phase. From these, the average lifetime of molecules in the surface is determined to be considerably longer than the inverse of the energy relaxation rate, so that the sticking coefficient is one and exiting molecules have no memory of their original velocities. However, most molecules do return to the gas phase rather than entering the bulk solution. The rate of passage of molecules over the free energy barrier is studied using the reactive flux method with trajectories initiated near the top of the barrier. The results for nitrogen, in particular, give a good plateau in the time-dependent transmission coefficient and hence a reliable rate constant. The results from these two sets of simulations are combined to give an effective interface width which is used to determine the permeability of thin water films. These results are compared to experimental permeabilities of thin Newton black soap films. The rate-determining step for solution in bulk water is not passage through the few Ångströms width of the interface we study, but rather the transport from the vicinity of the interface into the bulk over the larger distance scale of  $\mu\text{m}$ . © 1999 American Institute of Physics. [S0021-9606(99)71029-9]

## I. INTRODUCTION

The process of solution of molecules such as CO<sub>2</sub> and N<sub>2</sub> in water is important in many contexts, ranging from the production of bubbles when a champagne bottle is opened to the extent to which the oceans can act as a sink for CO<sub>2</sub>. Recent experiments<sup>1–3</sup> have addressed the problem of measuring the rate of solution of small molecules in liquids both macroscopically and with molecular beams.

In this paper we describe the results of simulation studies of this process. Atomistic simulation is appropriate for the investigation of the passage of molecules across the interface, as the width of the interface region is the order of magnitude of a few intermolecular spacings, which is accessible to simulation.

The thermodynamics of solution is determined by the free energy, energy, and entropy profiles of the system as a solute molecule crosses the interface. While the kinetics is not completely determined by the thermodynamics, these

profiles have a profound effect on them. In Fig. 1 we reproduce graphs showing the density of water across its liquid–vapor interface, and free energy profiles at 300 K for CO<sub>2</sub> and N<sub>2</sub> traversing the interface which were determined in previous simulations of solute molecules and thin films of water.<sup>4</sup> The dashed line in the figure shows the water density for one-half of the film (the position  $z=0$  corresponds to the center of the simulated film). The water density is slightly enhanced just below the interface and then drops to a negligible value as the interface is traversed from liquid to vapor. The width of the interface is about 4–5 Å. The free energy curves (in which the common zero corresponds to the solute in the gas phase) show that the influence of the interface on the solvation process extends over a wider region (10–14 Å). The equilibrium solute concentration  $c^{\text{eq}}(z)$  also varies over this wider region, as at any point  $z$  it is determined by

$$A(z) = -RT \ln [c^{\text{eq}}(z)/c_{\text{gas}}^{\text{eg}}], \quad (1.1)$$

where the concentrations are measured in moles per unit volume and  $c_{\text{gas}}^{\text{eq}}$  is the concentration of the solute in the gas phase. It follows that the value of the Ostwald solubility  $L$  is given by

<sup>a)</sup>Present address: Department of Chemistry, UMIST, Manchester M60 1QD, United Kingdom.

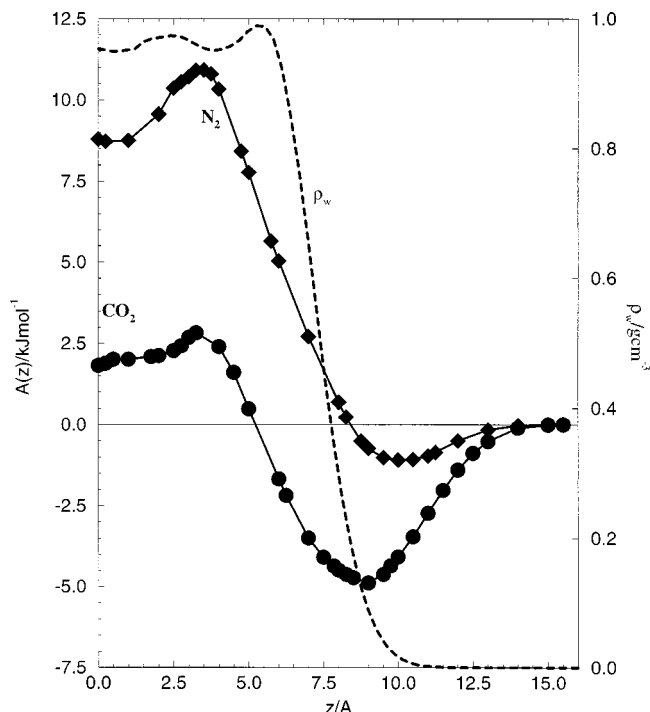


FIG. 1. Free energy profiles for CO<sub>2</sub> and N<sub>2</sub> traversing the interface. The dashed line shows the density of the water through the interface. Distances are measured from the center of the simulated film.

$$L = c_{\text{bulk}}^{\text{eq}}/c_{\text{gas}}^{\text{eq}} = \exp[-A_{\text{bulk}}/RT], \quad (1.2)$$

where  $A_{\text{bulk}}$  is the limiting value of the free energy  $A(z)$  on the liquid side of the interface and  $c_{\text{bulk}}^{\text{eq}}$  is the equilibrium concentration of the solute in the liquid. For both solutes considered here, the free energy has a minimum on the vapor side of the water surface and a small barrier between the bulk liquid and the surface. These minima correspond to regions in which the equilibrium solute concentration is enhanced. We deduce that both gases, but particularly CO<sub>2</sub>, form a surface-adsorbed layer in which solute molecules lie on the water surface, and have a significant surface excess concentration.

These free energy profiles suggest that the process of solution of these gases should be considered as a two-step process in which the molecules first move from the gas phase to the surface to form an adsorbed layer and then move from the adsorbed layer into the bulk. The passage of a gas molecule through a film consists of five steps, gas–surface, surface–bulk, diffusion through the bulk, bulk–surface, and finally surface–gas on the far side of the film. The two steps at the interface are very different in character from each other. In the first step (gas–surface), the solvent density is low and the solute motion is gaslike with a mean free path much greater than the distances considered here. In the second step (surface–bulk), the density of water rapidly increases to that of the bulk, and molecular motion becomes increasingly interrupted by solvent–solute interactions.

In this paper we present the results from a number of complementary simulation methods to determine the kinetics involved in the different steps outlined above. The gas–surface process was studied by following trajectories of the

TABLE I. Potential parameters.

Molecule	Site	$\epsilon_{iO}/\text{kJ mol}^{-1}$	$\sigma_{iO}/\text{\AA}$	$q/e$
CO <sub>2</sub>	C	0.5137	3.2618	0.6630
	O	0.8106	3.0145	-0.3315
N <sub>2</sub>	N	0.5050	3.282	-0.4731
	center	0.0	0.0	0.9462
H <sub>2</sub> O	H	...	...	0.4238
	O	0.6502	3.166	-0.8476

solute molecule moving from the gas phase toward the surface of a film of water at 300 K. This work and its results are described in Sec. III. The main conclusions are that incoming molecules are trapped on the surface in the free energy well where they are rapidly thermalized, and that the sticking coefficient is equal to unity.

The process of passing over the barrier from the surface into the bulk has been studied in two ways. First, by following the fate of the molecules trapped in the adsorption site (see Sec. III), and second, by following trajectories of molecules which were initially placed at the barrier and applying the reactive flux method. This is described in Sec. IV.

Passage through the region of a film which has bulk liquid properties is described by the diffusion equation as the molecules lose memory of their velocities before they move a significant distance. The diffusion of CO<sub>2</sub> and N<sub>2</sub> in bulk water was investigated by us in earlier work<sup>5,6</sup> using the same potential models, and good agreement with experimental values was found. We have also investigated the extension of this macroscopic approach to part of the interface region using the free energy  $A(z)$  as an external potential. This is described in Sec. V.

Finally, the results from the different simulation methods are brought together so that the permeation of CO<sub>2</sub> through films (Sec. V) and the rates of solution of CO<sub>2</sub> in water (Sec. VI) can be described and discussed. These methods give consistent results for the liquid–surface kinetics, although the uncertainties are large.

## II. MODELS AND METHODS

All the simulations were performed using the method of molecular dynamics. The DL\_POLY program<sup>7</sup> was adapted for the particular simulations. The simulation cell was the same as used in earlier work.<sup>4</sup> It contained a slab of liquid water about 15 Å thick with gas above and below. This cell was periodically repeated in space.

The water was modeled by the SPC/E model,<sup>8</sup> in which the geometry is fixed and there are partial charges on each atom site. In addition, every pair of oxygen atoms interacts with a Lennard-Jones potential. The water–CO<sub>2</sub> and water–N<sub>2</sub> interactions were modeled using a similar philosophy with partial charges on each atomic site (and an additional site at the center of the N<sub>2</sub> molecule), together with Lennard-Jones potentials between each atomic site and each water–oxygen. Table I gives values for the potential parameters. These were the same as in our earlier work<sup>4–6</sup> and were found to give good agreement with bulk thermodynamics

and diffusion constants. The long-range Coulomb terms were treated using Ewald summation with the parameters used previously.<sup>4</sup> A time step of 2 fs was used.

Simulations were initiated with the center of mass of the solute at a particular point and trajectories followed until the solute reached a predetermined point or a specified time interval had passed. In the gas–liquid trajectories, which were run at constant energy, the initial position of the center of mass of the solute was at 15 Å from the center of the film, which is about 7.5 Å from the midpoint of the interface (see Fig. 1). In order to conserve momentum and increase the efficiency of the calculations, trajectories were initiated with a pair of molecules on opposite sides of the film approaching the surfaces with equal and opposite velocities. Their trajectories were followed for 25 ps (sometimes longer) or until both molecules had left the interface region (defined for this purpose as being between 3.5 and 13.25 Å). Occasional trajectories had to be stopped when one solute molecule moved through the boundaries to reach the image of the other side of the film. Information from these trajectories was included in the analysis to prevent bias. In all, 285 trajectories for CO<sub>2</sub> and 173 for N<sub>2</sub> were run. Typical trajectories lasted for 10–40 ps.

The liquid–surface trajectory calculations were performed with a Nosé–Hoover thermostat with time constant of 0.4 ps. Trajectories were initiated with the center of mass of the solute at a point near the tops of the respective barriers (4 for CO<sub>2</sub> and 3 Å for N<sub>2</sub>). Our earlier work<sup>4</sup> showed periods of about 300 ps were sometimes necessary to sample a full range of configurations consistent with a particular constrained center of mass position. In order to obtain a thermal distribution of independent starting configurations, these were taken at intervals during a 7.5 ns run with a fixed solute center of mass at 300 K. About 800 trajectories were run for each solute. Typically each trajectory was followed for 4 ps.

### III. FROM GAS TO SURFACE

In this section we describe the results of trajectory calculations initiated in the gas phase. Figure 2 shows the decay of the number of trajectories in which solute molecules remain in the surface region as a function of time. The curves for both N<sub>2</sub> and CO<sub>2</sub> decay exponentially after the first few ps. The reason that the first 3–4 ps of these curves do not fall on the exponential decay is because the time origin is when the CO<sub>2</sub> is above the surface (at  $z = 15$  Å), and before it can escape it must reach the surface, interact, and move out again beyond the boundary of the surface region. At 300 K the average forward velocity is about 2 Å/ps (200 m/s) for CO<sub>2</sub>. The decay times obtained from the exponential fits are given in Table II for both CO<sub>2</sub> and N<sub>2</sub>. The lifetime of a CO<sub>2</sub> molecule adsorbed on the surface is about 15 ps, while that of N<sub>2</sub> is much shorter, about 3 ps.

A very important parameter in the discussion of kinetics of solution is the value of the sticking coefficient, that is the number of molecules which stay on the surface rather than immediately bouncing off it. Our conclusion is that the sticking coefficient is one, although most of the molecules which stick eventually escape back to the gas phase. This conclusion is based on the facts that first, at short times the number

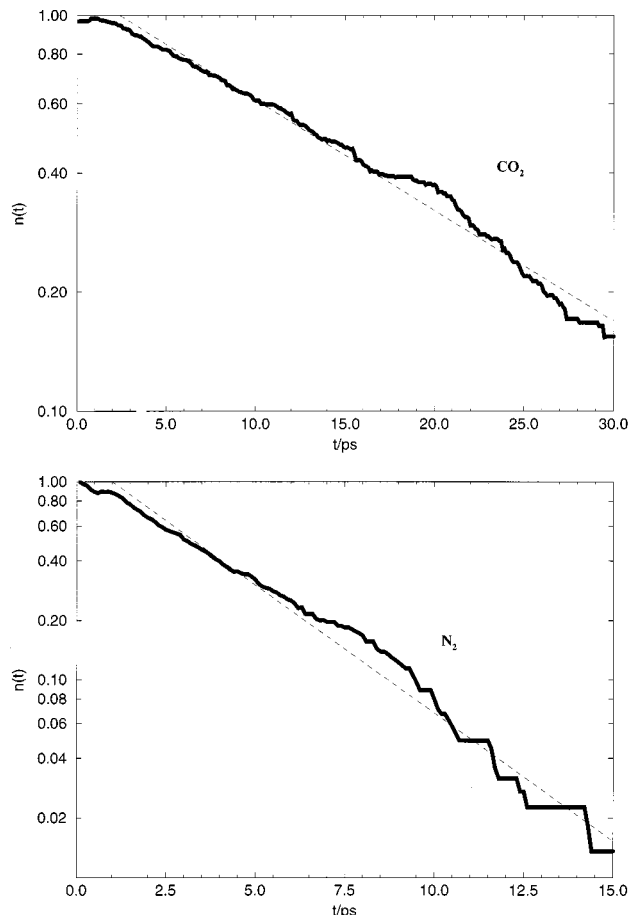


FIG. 2. Decay of number of solute molecules in the surface layer as a function of time (a) CO<sub>2</sub>; (b) N<sub>2</sub>.

of molecules leaving the surface is not higher than the fitted exponential decay (see Fig. 2), and second, that the rate of thermalization occurs on a faster time scale than the lifetime of the adsorbed molecules. This point is illustrated in Fig. 3, which shows the change in average translational kinetic energy for three series of trajectories in which the initial velocity of the CO<sub>2</sub> molecule approaching the film is different from that which would be expected from a thermal distribution at 300 K. After only 2 ps from the start of the trajectories, the average translational kinetic energy has reached the value for thermal equilibrium (3.74 kJ mol<sup>-1</sup> at 300 K), while only 2% of the molecules have escaped from the surface. The rate constants for thermalization of the incoming molecules can be found by fitting the decay after an initial delay for the molecules to reach the surface to an exponential. The resulting time constant is 0.3 ps, which is much shorter than the residence time on the surface.

The second important parameter needed for the description of the kinetics of crossing the interface is the fraction  $f$  of molecules leaving the surface which end in the bulk, as opposed to those which return to the gas phase. This number cannot be obtained from thermodynamic arguments and must be measured in kinetic experiments such as these. The value of  $f$  could be determined reasonably accurately for CO<sub>2</sub>, but too few molecules of N<sub>2</sub> reached the interior to give anything

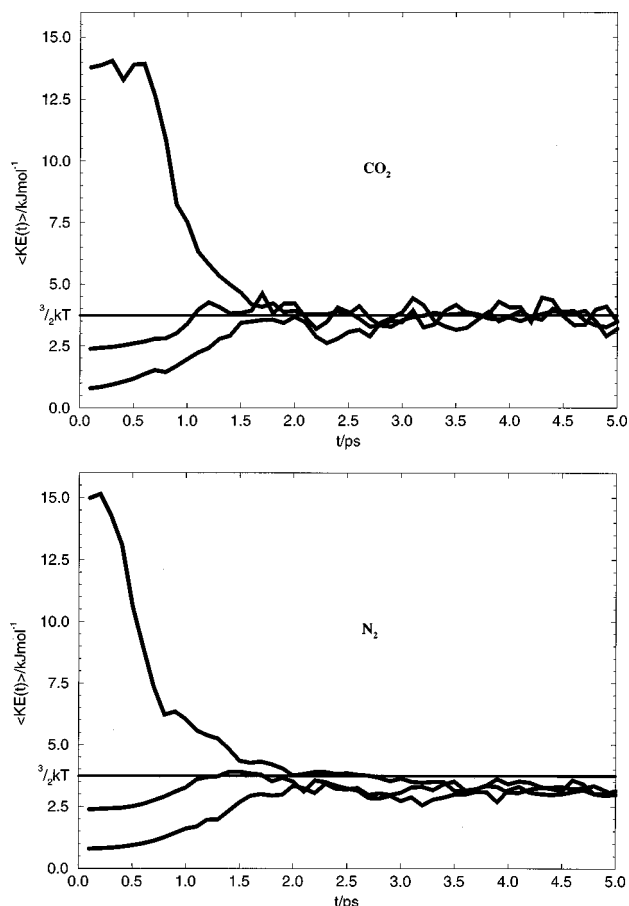


FIG. 3. Change of average translational kinetic energy of incoming solute molecules as a function of time. (a) CO<sub>2</sub>; (b) N<sub>2</sub>.

but a very uncertain estimate of  $f$  for N<sub>2</sub>. The results from this section are summarized in Table II.

Figure 4 gives some more detailed information about the dynamics of the solute in the interface region. It shows histograms of the number of solute velocity reversals as a function of solute position. Velocity reversals are defined as points at which the  $z$  component of the solute velocity changes sign. The dashed line shows the total number of reversals at different positions, while the two full curves show the numbers toward and away from the bulk liquid. This figure illustrates the contrast between motion in a potential well and in a free energy well. In the former, all velocity reversals to the right of the minimum would be toward the left, while those to the left of the minimum would be toward the right. In a free energy well such as in this system, interactions are more random and velocity reversals in either direction occur on both sides of the minimum, but relative numbers change as one goes through the minimum. Note that the curves cross near the free energy minimum, whose position is shown by the line S.

TABLE II. Results from gas to surface trajectories.

Solute	Lifetime in surface/ps	KE relaxation time/ps	Fraction $f$ to bulk
CO <sub>2</sub>	15.5±0.3	0.3±0.05	0.10±0.02
N <sub>2</sub>	3.3±0.2	0.4±0.05	0.009±0.008

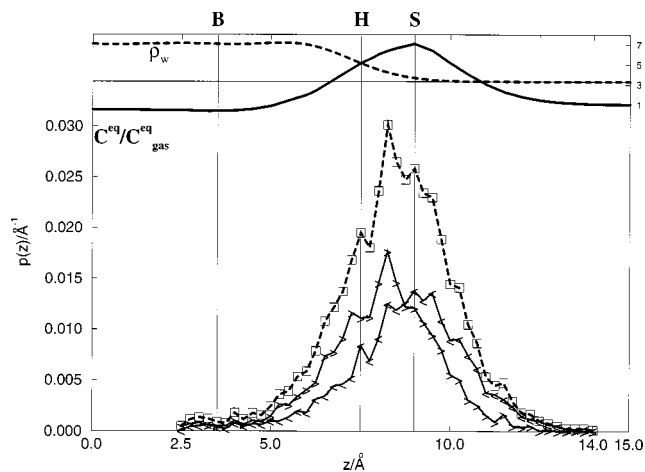


FIG. 4. Histograms of velocity reversals of a CO<sub>2</sub> molecule as a function of position. The dashed line shows the total number, while the two full lines with symbols  $\langle$  and  $\rangle$  show reversals from right to left and from left to right, respectively. The water density and equilibrium solute concentrations are shown above for reference. Note that more reversals from left to right occur when the solute is outside the free energy minimum (S) and vice versa.

The overall picture is then that the incoming molecules strike the surface and stick in the adsorbed layer where they quickly lose memory of their original velocity and kinetic energy. After several picoseconds, the thermalized molecules escape either into the bulk with probability  $f$  or back into the gas phase with probability  $(1-f)$ .

#### IV. PASSAGE OVER THE BARRIER

The use of molecular dynamics to study rates of crossing activated barriers in chemical reactions is well established. In the reactive flux method,<sup>9</sup> trajectories are initiated at the barrier and the probability of finding the system on the product side at later times monitored. This method can be used for the current problem to investigate the rate constants for passage over the barriers which lie between the liquid and the surface. These barriers are comparatively low compared with most chemical reactions and it is not clear *a priori* that a rate constant exists, particularly for the CO<sub>2</sub> where the barrier is  $0.5 kT$ . In fact we do find rate constants for both solutes.

Using the ideas of transition state theory we can calculate the flux  $J_{LS}$  from liquid to surface per unit area across a plane parallel to the surface and passing through the barrier. At thermal equilibrium the flux is the product of the number density of molecules at the barrier, their mean forward velocity  $\langle |v_z| \rangle / 2$ , and a transmission function  $\kappa$ . As the equilibrium concentration of molecules at the barrier,  $c_B^{eq}$  is related to that in the bulk fluid  $c_L^{eq}$  by

$$c_B^{eq} = c_L^{eq} \exp[-(A(z_B) - A_{liq})/kT], \quad (4.1)$$

the flux across the barrier at equilibrium from liquid to surface is

$$J_{LS} = k'_{LS} c_L^{eq} = \exp[-(A(z_B) - A_{liq})/kT] \langle |v_z| \rangle / 2 \kappa c_L^{eq}, \quad (4.2)$$

where the rate constant  $k'_{LS}$  has units of a velocity. We adopt the convention that rate constants without primes have dimensions of inverse time while those with primes have dimensions of velocity. In this expression all the variables ex-

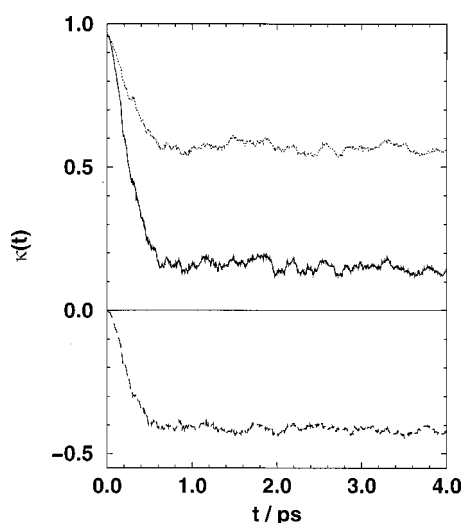


FIG. 5. Time dependence of the transmission function (continuous line) for  $N_2$  for trajectories initiated at  $z = 3 \text{ \AA}$ . The dotted and dashed lines show the contributions of trajectories which start with forward velocities (dotted, above) and backward velocities (dashed, below). Note that a plateau is reached after 0.5 ps.

cept  $\kappa$  can be determined from equilibrium statistical mechanics. In the transition state approximation  $\kappa$  is equal to one. This assumes that no trajectories recross the barrier; in general,  $\kappa$  is less than one to correct for recrossings. The determination of  $\kappa$  from trajectory calculations has been described by Chandler.<sup>9</sup> In our case the reaction coordinate is the  $z$  position of the center of mass of the solute molecule. The flux of molecules crossing a plane perpendicular to the  $z$  axis at a point  $z_0$  on the reaction path is given by

$$J = c(z_0) \langle v(t=0) H(z(t) - z_0) \rangle, \quad (4.3)$$

where the average is taken over trajectories whose initial positions at  $t=0$  are  $z=z_0$ .  $H(z)$  is the Heaviside function whose value is 0 for a negative argument and 1 for a positive argument. Comparing this expression for the flux with Eq. (4.2), we obtain

$$\kappa(z_0, t) = \frac{\langle v(t=0) H[z(t) - z_0] \rangle}{\langle |v_z|/2 \rangle}. \quad (4.4)$$

If  $\kappa$  reaches a plateau value after a short time, the process can be described by first-order kinetics, and a rate constant exists. Thus from Eq. (4.2) we obtain

$$k'_{LS} = \kappa(z_0) \exp[-(A(z_0) - A_{\text{bulk}})/kT] \langle |v_z|/2 \rangle, \quad (4.5)$$

where  $\kappa$  is determined from reactive flux calculations,  $A(z_0) - A_{\text{bulk}}$  from our earlier free energy measurements, and  $\langle |v_z|/2 \rangle = (kT/2\pi m)^{1/2}$ . It should be noted that Eq. (4.3) is valid at all values of  $z_0$ , changes in  $c(z_0)$  being compensated by changes in  $\kappa(z_0)$ . However, as  $z_0$  moves away from the top of the barrier, the concentration increases rapidly and the values of  $\kappa$  become close to zero. Consequently, accurate values are difficult to obtain unless trajectories are started near the top of the barrier.

Figure 5 shows  $\kappa(t)$  for  $N_2$  starting at  $z = 3 \text{ \AA}$ , near the top of the barrier. It is clear that a plateau is reached after about 0.6 ps and the plateau value of  $\kappa$  is  $0.15 \pm 0.02$ . This

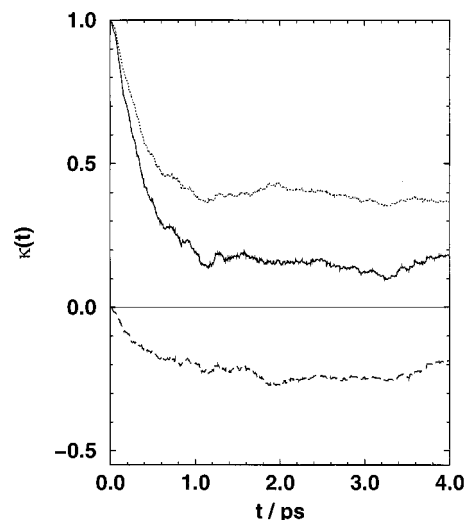


FIG. 6. Time dependence of the transmission function (continuous line) for  $CO_2$  for trajectories initiated at  $z = 4 \text{ \AA}$ . The dotted and dashed lines show the contributions of trajectories which start with forward velocities (dotted, above) and backward velocities (dashed, below). Compared to nitrogen the plateau is less well defined.

substantial reduction from unity shows that barrier recrossings are common. As a result, both forward and backward trajectories contribute to the value. These two terms are shown separately in the figure and contribute about equally to the decay of  $\kappa$  from unity. This is further evidence for multiple barrier crossing.

The results for  $CO_2$  were more noisy and are shown in Fig. 6 for trajectories starting from  $z = 4 \text{ \AA}$ . This is a point on the surface side of the barrier. The plateau value at about 2 ps gives  $\kappa = 0.15 \pm 0.04$ .

Using these values of  $\kappa$  and the values of the free energy at the corresponding starting points, we obtain values for the rate constants from liquid to surface of

$$k'_{LS} = 0.08 \pm 0.02 \text{ \AA ps}^{-1} N_2,$$

$$k'_{LS} = 0.10 \pm 0.08 \text{ \AA ps}^{-1} CO_2.$$

## V. RATES OF PERMEATION OF FILMS

We have seen that the passage of a molecule through a film is made up of several steps, namely reaching the surface, passing through the interface, moving through the central part of the film which has bulk properties, passing through the far interface, and leaving the surface. We have already discussed the surface and interface processes. The movement of  $CO_2$  and  $N_2$  through the central portion of the film can be described by the diffusion equation, provided that the thickness of the film is considerably greater than the amplitude of motion of a molecule in its cage. For a thick film, it is this process that limits the permeation so that the rate is inversely proportional to the film width. We shall show in this section that the effects of the interfaces can be described in terms of an effective interface width (which may be negative) which should be added to the true film width to determine the effective width. We compute values of this correction for  $CO_2$  and  $N_2$ .

Fick's law states that

$$J = -D \frac{dc}{dz}, \tag{5.1}$$

so that the concentration is a linear function of  $z$  under steady-state conditions where  $J(z,t)$  is constant, giving

$$c(z_1) - c(z_2) = \frac{J}{D} (z_1 - z_2). \tag{5.2}$$

The crudest model for permeation through a film is one where the interfaces at  $\pm h/2$  are sharp and the concentrations just inside the interfaces are in equilibrium with the neighboring gas. Assuming that the gas-phase pressure on each side (and hence the concentrations) are kept constant, we have

$$J = \frac{DL}{h} [c_{\text{gas}}(1) - c_{\text{gas}}(2)], \tag{5.3}$$

where  $L$  is the Ostwald solubility of the gas defined in Eq. (1.2). This can be rewritten (assuming the gases are ideal),

$$J = \frac{DL}{hkT} [p_{\text{gas}}(1) - p_{\text{gas}}(2)]. \tag{5.4}$$

The effects of the processes at the interfaces modify these equations so that the width of the film  $h$  is replaced by an effective width  $h_{\text{eff}} = h + 2\Delta$ . The interface correction,  $\Delta$ , is the same for films of all widths, but will only be significant when the interface correction is a similar order of magnitude as the film width. This correction may be positive or negative depending on the properties of the solute and the interface. Once its value has been determined for a particular solute/solvent combination, we can estimate the permeation of films of any thickness.

Our next task is to combine the information from the simulations described in earlier parts of this paper and previous papers<sup>4-6</sup> in order to estimate  $\Delta$  for CO<sub>2</sub> and N<sub>2</sub> crossing the water gas-liquid interface at 300 K.

Figure 7 shows the water density in the film (above) and the free energy  $A(z)$  (below) schematically. We define the true film width  $h$  as being the distance between the points  $H_1$  and  $H_2$  in the interface where the density is half the liquid density in the interior of the film. The positions of the barriers,  $B_1$  and  $B_2$ , and the limits of bulk behavior,  $L_1$  and  $L_2$ , lie within the film.  $a$  is the distance between the limit of bulk behavior and the edge of the film. We assume that solute is flowing from left to right in a steady state so that the flux  $J$  is constant throughout the film. Thus the values of  $J$  across different planes  $P_1$ ,  $B_1$ ,  $B_2$ , and  $P_2$  perpendicular to  $z$  can be equated to obtain expressions for the overall permeation rate. The flux across the plane  $P_1$  between the gas phase ( $G_1$ ) and the surface adsorbed layer ( $S_1$ ) is

$$J = \langle |v_z|/2 \rangle c_{G1} - k_{SG}' c_{S1}', \tag{5.5}$$

where we have used the observation that the sticking coefficient is equal to one. In this expression  $c_{S1}'$  is the surface concentration in the adsorbed layer  $S_1$  and  $c_{G1}$  the volume concentration in the gas phase  $G_1$ .

The flux across barrier  $B_1$  is

$$J = k_{SL}' c_{S1}' - k_{LS}' c_{L1}, \tag{5.6}$$

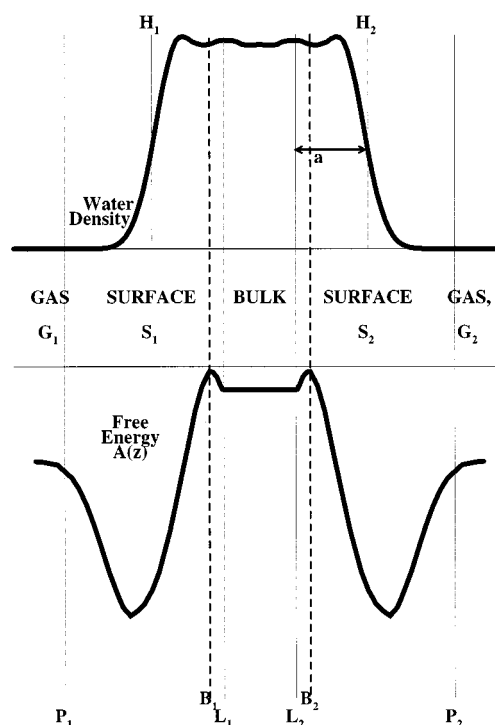


FIG. 7. Schematic diagram of the film and its associated free energy profile showing different planes and regions of the film.

where  $c_{L1}$  is the concentration just inside the barrier and the rate constants between liquid and surface ( $k'_{LS}$ ) and surface and liquid ( $k_{SL}$ ) have dimensions of velocity and inverse time, respectively. Combining Eqs. (5.5) and (5.6), the corresponding equations for the fluxes across planes  $B_2$  and  $P_2$ , and the solution of the diffusion equation for the flux in the interior of the film, we obtain

$$J = D(c_{L1} - c_{L2})/[z(L1) - z(L2)]. \tag{5.7}$$

The steady-state concentrations in the surfaces and the interior can be eliminated to give

$$J = DL(c_{G1} - c_{G2})/h_{\text{eff}}. \tag{5.8}$$

This equation has the expected form [cf. Eq. (5.3)]. By manipulation we obtain two independent expressions for the effective film width of the form

$$h_{\text{eff}} = z(L1) - z(L2) + 2\delta, \tag{5.9}$$

namely

$$\delta = \frac{DL}{f\langle |v_z|/2 \rangle} \text{ ‘‘surface equation’’}, \tag{5.10}$$

$$\delta = \frac{D}{k'_{LS}(1-f)} \text{ ‘‘barrier equation’’}, \tag{5.11}$$

where  $f$  is the fraction of trajectories starting from the surface adsorbed phase which enter the bulk and  $(1-f)$  is the fraction that escape to the gas phase. The other quantities have been defined before. We note that the first of these equations (the ‘‘surface’’ equation) depends primarily on information from the trajectories initiated in the gas phase, while the

TABLE III. Data for model and experiment.

Solute		Diffusion const. $D/\text{\AA}^2 \text{ps}^{-1}$	Solubility $L$	Film edge $H/\text{\AA}$	Barrier $B/\text{\AA}$	$A(z_0) - A_{\text{bulk}}$ $/\text{kJ mol}^{-1}$
CO <sub>2</sub>	model <sup>a,b</sup>	0.18±0.02	0.45±0.04	7.4	3.3±0.1	0.8±0.2
	expt. <sup>c,d,e</sup>	0.20	0.80			
N <sub>2</sub>	model <sup>a,f</sup>	0.20±0.04	0.030±0.003	7.4	3.4±0.1	2.1±0.2
	expt. <sup>c,d,g</sup>	0.23	0.016			

<sup>a</sup>Reference 4.<sup>e</sup>Reference 26.<sup>b</sup>Reference 5.<sup>f</sup>Reference 6.<sup>c</sup>Reference 23.<sup>g</sup>Reference 25.<sup>d</sup>Reference 24.

second (the ‘‘barrier’’ equation) depends primarily on information from the trajectories initiated on the barrier.

The other information we require is the offset  $a$  (see Fig. 7) of the points  $L1$  and  $L2$  just inside the barrier from the edge of the interface defined by the point at which the water density is 50% of its value in the center of the film. The points  $L1$  and  $L2$  are not precisely determined, but from the free energy curves (Fig. 1) we estimate

$$z(L1) - z(L2) = h - (10 \pm 1) \text{\AA} \text{ CO}_2, \quad (5.12)$$

$$z(L1) - z(L2) = h - (12 \pm 1) \text{\AA} \text{ N}_2. \quad (5.13)$$

Thus the offsets are  $a = 5 \pm 0.5 \text{\AA}$  for CO<sub>2</sub> and  $a = 6 \pm 0.5 \text{\AA}$  for N<sub>2</sub>. These quantities are the least accurately determined contributions to the interface correction, as the precise point at which the properties of the solution are the same as those of the bulk is not well determined.

The remaining quantities needed to determine  $\Delta$  from our previous work<sup>4-6</sup> and experiment are collected in Table III. Table IV shows the results of calculating  $\delta$  from the two routes [Eqs. (5.10) and (5.11)], together with our estimates of the total interface correction  $\Delta = \delta - a$  for the gases passing through the gas-liquid interface of water. Values have been calculated with all parameters taken from the model with experimental values of  $D$  and  $L$  (rows labeled ‘‘model’’ and ‘‘corr,’’ respectively). Although the values of  $\delta$  for CO<sub>2</sub> agree within their estimated errors, the difference between the values of  $\delta$  is significant owing to the low value of the solubility of the model CO<sub>2</sub> compared to the experimental value. It should be noted that this difference in solubility corresponds to a difference of 1.5 kJ mol<sup>-1</sup>, which is not large. The ‘‘surface’’ equation gives a more precise value for CO<sub>2</sub>, while for N<sub>2</sub>, where the value of  $f$  is too small to be determined accurately from the gas to surface trajectories, the ‘‘barrier’’ equation is more accurate. The less accurate values are bracketed in the table.

We note that the total interface correction  $\Delta$  is negative, showing that it is easier to pass through the interface than through an equivalent distance of bulk water. Why is this? Although the existence of a barrier impedes the passage of the gas, this is more than compensated for by the attraction of the free energy minimum at the surface. This balance is illustrated by another expression for  $\Delta$  which is obtained from solving the diffusion equation in the presence of the mean force on the molecule due to the free energy  $[-dA(z)/dz]$ ,

$$\Delta_{\text{diff}} = \int_{z_S}^{\text{bulk}} \frac{1 - \exp[-(A(z) - A_{\text{bulk}})/kT]}{D(z)/D} dz. \quad (5.14)$$

The integral runs from the surface  $z_S$  into the bulk liquid. Regions where the free energy is lower than in the bulk give negative contributions, while the barrier region where  $A(z) > A_{\text{bulk}}$  gives a positive contribution to the value of  $\Delta$ . The main problems with applying this approach in a quantitative manner is that the diffusion constant  $D(z)$  is expected to drop rapidly through the interface and it is doubtful whether the conditions for validity of the diffusion equation are met in this region. Nevertheless we include values estimated from this equation in the last column of Table IV.

## VI. RATES OF SOLUTION IN LIQUIDS

There have been various types of experimental studies of the rate of solution of CO<sub>2</sub> in water. In the more traditional methods, the rate of solution into bulk liquid has been studied with various arrangements including flowing and stirred liquids,<sup>2,3,10</sup> while Davidovits *et al.*<sup>11</sup> have developed an ingenious method of studying the absorption of highly soluble gases in small droplets of the order of 0.1 mm in diameter.

TABLE IV. Calculation of  $\Delta$  (see text).

Solute		$\langle  v_z/2  \rangle$ $/\text{\AA} \text{ps}^{-1}$	$k'_{LS}$ $/\text{\AA} \text{ps}^{-1}$	$\delta(\text{barrier})$ $/\text{\AA}$	$\delta(\text{surface})$ $/\text{\AA}$	offset $a$ $/\text{\AA}$	$\Delta$ $/\text{\AA}$	$\Delta$ (diffusion)
CO <sub>2</sub>	model	0.95	0.10±0.08	(2.0±1.6)	0.9±0.2	5±0.5	-4.1±0.7	(-2.2)
	corr.			(2.2±1.6)	1.7±0.4		-3.3±0.9	
N <sub>2</sub>	model	1.19	0.08±0.02	2.8±0.7	(0.6±0.5)	6±0.5	-3.0±1.0	(0.3)
	corr.			2.9±1.0	(0.3±0.3)		-3.1±1.0	



The study of scattering and absorption of molecular beams from liquid surfaces provides a complementary view of the problem.<sup>1,12</sup>

Experimentally, the solution of gases in liquids has been found to be a first-order process in which the net flux of material from the gas phase into liquid is described by the equation

$$J = k'_{\text{exp}}(c_{\text{bulk}}^{\text{eq}} - c_{\text{bulk}}), \quad (6.1)$$

where  $k'_{\text{exp}}$  is a rate constant with dimensions of a velocity and  $c_{\text{bulk}}$  is the actual concentration of the gas in the liquid. Although the value of the rate constant depends on the rate of stirring of the solution, Noyes *et al.*<sup>2</sup> found that it reached a plateau value at moderate stirring rates; further increases were attributed to vortexing. They evaluated the accommodation coefficient,  $\gamma$  (defined as the probability that a molecule hitting the surface reaches the bulk), using the plateau value of the rate constant. They found that the accommodation coefficient for CO<sub>2</sub> entering pure water was found to be  $\gamma = (5.4 \pm 0.4) \times 10^{-8}$  at 25 °C, that is only two molecules in a thousand million which hit the surface reach the bulk liquid. This number is orders of magnitude smaller than the values either of the sticking coefficient ( $=1$ ) or the fraction of molecules passing through the interface ( $f \approx 0.1$ ) measured in these simulations. This shows that the rate-determining step for solution in bulk liquid is neither the initial collision with the surface nor the passage through the interface. It has been generally recognized that the transport of the molecules from the interface into the bulk is important. There have been a number of models proposed for this process. The simplest of these is the stagnant layer model,<sup>13</sup> in which the rate-determining process is the diffusion through a stagnant layer which is not affected by stirring. Using our results and the experimental value of  $\gamma$  it is possible to estimate the thickness of such a layer.

From an analogous treatment to that used to obtain the rate of permeation for films in Sec. V, we obtain an expression for the steady-state flux through the interface and stagnant layer

$$J = \frac{D}{h_{\text{stag}} + \delta} (c_{\text{bulk}}^{\text{eq}} - c_{\text{bulk}}), \quad (6.2)$$

where  $h_{\text{stag}}$  is the width of the stagnant layer and  $\delta$  is the quantity associated with the interface defined in Eqs. (5.10) and (5.11). As the flux onto the surface is given by

$$J_{\text{on}} = \langle |v_z|/2 \rangle c_{\text{gas}}, \quad (6.3)$$

$\gamma$  is given by

$$\gamma = J/J_{\text{on}} = \frac{DL}{\langle |v_z|/2 \rangle (h_{\text{stag}} + \delta)}. \quad (6.4)$$

Thus

$$h_{\text{stag}} + \delta = \frac{LD}{\langle |v_z|/2 \rangle \gamma}, \quad (6.5)$$

which for CO<sub>2</sub> using the experimental values of  $L$ ,  $D$ , and  $\gamma$ , gives

$$h_{\text{stag}} + \delta = 0.3 \text{ mm}, \quad (6.6)$$

showing that the interface term,  $\delta$ , is negligible.

In the renewal theory of the rate of gas absorption,<sup>10,14</sup> it is supposed that the layer of liquid just below the interface is mixed with the bulk from time to time. We can make no comment on this theory from our simulations.

## VII. DISCUSSION AND CONCLUSIONS

In this paper we have presented results from simulations of carbon dioxide and nitrogen in and near thin films of water which give quantitative information about the processes involved in dissolving these gases in liquid water. Although the liquid–gas interface of water is about 5 Å wide as defined by density variations, it is much wider (10–15 Å) from the point of view of a solute molecule, which begins to interact with the liquid at some distance away in the gas phase and does not reach its bulk properties until it is far enough inside the liquid to form at least one complete solvation shell. The process of solution can be divided into two parts which we have studied separately. The initial encounter of the solute with the surface results in it sticking on the surface in a free energy minimum. For both the solutes considered here the molecule is less likely to penetrate into the bulk solution than to escape back into the gas phase, so the rate-determining step in the passage through the interface is the surface–liquid step. On the other hand, the subsequent diffusion of the molecule in the bulk liquid is more important in macroscopic problems.

The simulations all involved one or two solute molecules only, and have been carried out at 300 K. Thus effects of concentration and temperature have not been investigated. However, at 1 atmosphere pressure, only  $2.5 \times 10^{-5}$  carbon dioxide molecules hit each square Ångstrom of surface every picosecond. Using the numbers in the table this gives an equilibrium concentration of  $3.2 \times 10^{-4}$  molecules per square Ångstrom in the adsorbed layer. The average separation of these surface-adsorbed molecules ( $\approx 50$  Å) is greater than the width of our simulation cell (14.7 Å) and is large enough that interactions between molecules is unlikely to be important.

The most direct application of these results would be to permeation of thin films of pure water under steady-state conditions. Such films are unstable and have not been investigated experimentally. The stability of thin water films is greatly enhanced by the presence of surfactant monolayers. The permeation rates of thin soap films have been thoroughly investigated; see, for example, the review by Exerowa *et al.*<sup>15</sup> It was established that the permeability is dependent on temperature, the type of electrolyte, type of surfactant, and their concentrations.<sup>16–21</sup> The thinnest soap films, known as Newton black films, consist of two surfactant monolayers absorbed onto each other. Somewhat thicker thin soap films, for which the monolayers are separated by a water layer, are known as common black films. It has been found that the permeability of a typical Newton black film is usually larger than the permeability of a typical common black film.

Table V shows a comparison between the permeation rates of thin water films and a typical thin soap film. All the results are obtained under steady-state conditions at  $T = 300$  K. The thin soap film consists of two layers of surfactant back-to-back with width of about 60 Å. It will be seen

TABLE V. Experimental permeation rates for a thin Newton black soap film, and calculated rates for water films of width 150, 60, and 15 Å.

Solute	Soap	Water films		
	$k_{\text{expt}}/\text{m s}^{-1}$	$k(150)/\text{m s}^{-1}$	$k(60)/\text{m s}^{-1}$	$k(15)/\text{m s}^{-1}$
CO <sub>2</sub>	0.1	0.11	0.3	2.4
N <sub>2</sub>	0.0015	0.003	0.007	0.04

from the figures in the table that a water film is a factor of 2–4 times more permeable than the soap film of the same thickness. The water film thickness has to be increased to over 150 Å to give the same permeability. This is probably due to a lower solubility of the CO<sub>2</sub> in the alkyl chain region.

We have shown the feasibility of our approach for calculating permeation rates of films of any thickness under steady-state conditions. The rates of solution of gases in liquids is a more complex problem. Unlike most chemical reactions where passage goes from reactant to product, the passage of the gas through the interface is not the end of the story. Our simulations support the idea that it is the movement of the solute away from the surface that is usually rate-determining. This is affected by local conditions such as stirring (both in experiments and by ocean waves) and currents caused by convection and other processes. In the experimental method developed by Davidovits *et al.*,<sup>1</sup> the rate of gas uptake into small droplets of about 100 μm is measured. They have only published results on much more soluble gases than CO<sub>2</sub>, but the values of  $\gamma$  they find are nearer the order of magnitude that we calculated for  $f$  (e.g.,  $\gamma=0.1$  for dimethylsulfoxide in water at 273 K). This may be coincidental, as one expects larger values of  $f$  for more soluble gases, but it should be noted that the droplet size is comparable to the deduced thickness of the stagnant layer for water and processes of stirring and convection must be very different in micro-droplets and bulk liquids.

A more microscopic experimental investigation of the process of adsorption on and passage through the interface has been performed by Nathanson and colleagues (for a review see Ref. 22). They have used incident beams of molecules of known energy (ranging from  $kT$  to  $60kT$ ) scattering off a freshly made surface of a liquid and determined the velocity distribution of scattered molecules using time-of-flight measurements. In general, the results show two overlapping velocity distributions which are interpreted as representing direct scattering from hard-sphere-like collisions and trapping followed by thermalization and desorption, respectively. Their results show that there is a high probability of trapping when the incident molecules are already near thermal velocity. At higher incident velocities a prominent direct peak appears, which is attributed to hard-sphere-like collisions. Our results for incident molecules at thermal energies have a sticking coefficient of unity with all the molecules becoming thermalized before leaving. Even at incident energies up to  $5kT$  we saw no sign of directly scattered molecules. However, there are important differences between their experiments and our simulations. In the experiments the liquid must have a very low vapor pressure so as not to interfere with the incoming molecular beam. They note that

the fraction of molecules thermalized is lower if the gas molecules are light compared to the liquid molecules and if the incident beam has high energies and near glancing incidence. Our incident molecules are a factor of 2–3 more massive than the liquid molecules (water) and the impact direction in the gas–liquid trajectories is either perpendicular to the surface or at 54°. It is possible that the sticking coefficient will be reduced at much higher energies.

In this work we have used simulation methods to estimate free energies of CO<sub>2</sub> and N<sub>2</sub> molecules penetrating the surface of liquid water, the sticking probability of molecules incident from the gas phase ( $\sim 1$ ), the barrier transmission coefficient ( $\sim 0.15$ ), the lifetime of molecules adsorbed in the surface layer ( $\sim 15$  ps for CO<sub>2</sub>), and the fraction of adsorbed molecules which enter the bulk ( $\sim 0.1$  for CO<sub>2</sub>). We have used two different methods to estimate a correction to the permeability of a thin layer of water to CO<sub>2</sub> and N<sub>2</sub> molecules caused by a nonuniform layer at the liquid surface. Both methods agree as to the thickness of this layer. In each case the correction is negative, which means that a thin layer of water with this nonuniform surface layer is slightly more permeable than a sharply truncated bulk. However, the change in permeability caused by this layer, for all but the thinnest liquid layers, is relatively small.

Simulation results for the process of adsorption are similar to those found by molecular beam scattering experiments at liquid surfaces where molecules are observed to stick with a high probability and then mostly desorb again after thermalization is complete. Estimates of the permeation rate of thin films of water from the simulation results are similar to the experimental values found for permeation rates in thin soap films. Experimental measurements of the accommodation coefficient indicate that only a very small fraction of molecules incident on a water surface actually reach the true bulk. There are therefore other important processes which are rate-limiting in dissolution of small molecules in liquids.

## ACKNOWLEDGMENTS

We acknowledge the generous support of the Hitachi Dublin Laboratory, who provided computer time. M.i.h.P. acknowledges support from the EU Human Capital and Mobility Program under Contract No. ERBCHBGCT 940520 and Forbairt, and T.S. acknowledges support from Queen's University and the ESF. We thank the EPSRC (Grant Nos. GR/K20651 and GR/L08427) and the IFI (Grant to the Irish Center for Colloids and Biomaterials) for their financial support for this work.

<sup>1</sup>G. M. Nathanson, P. Davidovits, D. R. Worsnop, and C. E. Kolb, *J. Phys. Chem.* **100**, 13007 (1996).

<sup>2</sup>R. M. Noyes, M. B. Rubin, and P. G. Bowers, *J. Phys. Chem.* **100**, 4167 (1995).

<sup>3</sup>R. M. Noyes, M. B. Rubin, and P. G. Bowers, *J. Phys. Chem.* **96**, 1000 (1992).

<sup>4</sup>T. Somasundaram, R. M. Lynden-Bell, and C. H. Patterson, *Phys. Chem. Chem. Phys.* **1**, 143 (1999).

<sup>5</sup>M. in het Panhuis, C. H. Patterson, and R. M. Lynden-Bell, *Mol. Phys.* **94**, 963 (1998).

<sup>6</sup>M. in het Panhuis, Ph.D thesis, Trinity College, Dublin, 1998.

<sup>7</sup>T. R. Forester and W. Smith, *The DL-POLY-2.0 Reference Manual*, version 2.0 (CCLRC, Daresbury Laboratory, Warrington, England, 1995).

- <sup>8</sup>H. J. C. Berendsen, J. R. Grigera, and T. P. Straatsma, *J. Phys. Chem.* **91**, 6269 (1987).
- <sup>9</sup>D. Chandler, *Introduction to Modern Statistical Mechanics* (Oxford University Press, Oxford, 1987).
- <sup>10</sup>D. B. Moog and G. H. Jirka, *J. Hydr. Eng.* **125**, 3 (1999).
- <sup>11</sup>J. T. Jayne, P. Davidovits, D. R. Worsnop, M. S. Zahniser, and C. E. Kolb, *J. Phys. Chem.* **95**, 6329 (1991).
- <sup>12</sup>M. E. Saecker, S. T. Govoni, D. V. Kowalski, M. E. King, and G. M. Nathanson, *Science* **252**, 1421 (1991).
- <sup>13</sup>W. S. Broecker and T. H. Peng, *Tellus* **26**, 21 (1974).
- <sup>14</sup>P. V. Danckwerts, *Ind. Eng. Chem.* **43**, 1460 (1951).
- <sup>15</sup>D. Exerowa, D. Kashchiev, and D. Platikanov, *Adv. Colloid Interface Sci.* **40**, 201 (1992).
- <sup>16</sup>R. Krustev, D. Platikanov, and M. Nedyalkov, *Colloids Surf., A* **123–124**, 383 (1997).
- <sup>17</sup>R. Krustev, D. Platikanov, and M. Nedyalkov, *Colloids Surf., A* **79**, 129 (1993).
- <sup>18</sup>R. Krustev, D. Platikanov, and M. Nedyalkov, *Langmuir* **12**, 1688 (1996).
- <sup>19</sup>R. Krustev, D. Platikanov, A. Stankova, and M. Nedyalkov, *J. Disp. Sci. Tech.* **18**, 789 (1997).
- <sup>20</sup>M. Nedyalkov, R. Krustev, D. Kashiev, D. Exerowa, and D. Platikanov, *Colloid Polym. Sci.* **266**, 291 (1988).
- <sup>21</sup>M. Nedyalkov, R. Krustev, A. Stankova, and D. Platikanov, *Langmuir* **8**, 3142 (1992).
- <sup>22</sup>P. Davidovits, J. T. Jayne, S. X. Xuan, D. R. Worsnop, M. S. Zahniser, and C. E. Kolb, *J. Phys. Chem.* **95**, 6337 (1991).
- <sup>23</sup>H. M. Princen and S. G. Mason, *J. Colloid Sci.* **20**, 353 (1965).
- <sup>24</sup>H. M. Princen, J. Th. G. Overbeek, and S. G. Mason, *J. Colloid Interface Sci.* **24**, 125 (1966).
- <sup>25</sup>IUPAC, *Solubility Data Series*, edited by R. Battino (Pergamon, Oxford, 1982), Vol. 10.
- <sup>26</sup>IUPAC, *Solubility Data Series* (Oxford University Press, Oxford, 1996), Vol. 62.